

Multifractal Detrended Fluctuation Analysis of Sunspot Time Series

M. Sadegh Movahed^{1,2}, G. R. Jafari¹, Sohrab Rahvar^{1,2} and M. Reza Rahimi Tabar^{1,3},

¹*Department of Physics, Sharif University of Technology, P.O.Box 11365-9161, Tehran, Iran*

²*Institute for Studies in theoretical Physics and Mathematics, P.O.Box 19395-5531, Tehran, Iran*

³*CNRS UMR 6529, Observatoire de la Côte d'Azur, BP 4229, 06304 Nice Cedex 4, France*

We use the multifractal detrended fluctuation analysis (MF-DFA), to study the sunspot number fluctuations. We show that sunspot time series has a crossover time scale (s_{\times}), where the signal has different correlation exponents in time scales $s > s_{\times}$ and $s < s_{\times}$. Comparing the MF-DFA results of the original time series to those for shuffled and surrogate series, we conclude that its multifractality nature is almost due to long-range correlations.

PACS numbers: 05.45.Tp, 05.40.-a, 96.60.Qc

I. INTRODUCTION

Sunspots are observed as moderate-dark formations on the sun surface. A sunspot is a relatively cool area on the solar surface that appears as a dark blemish [1]. The number of sunspots is continuously changing in time in a random fashion and constitutes a typically random time series. Because of the symmetry of the twisted magnetic lines as the origin of sunspots, they are generally seen in pairs or in groups of pairs at both sides of the solar equator. As the sunspot cycle progresses, spots appear closer to the sun's equator giving rise to the so called "butterfly diagram" in the time latitude distribution. Figure 1 shows the monthly measured number of sunspots in terms of time. This plot includes 3077 data points. The data belongs to a data set collected by the Sunspot Index Data Center (SIDC) from 1749 up to now [2].

In recent years the detrended fluctuation analysis (DFA) method has become a widely-used technique for the determination of (mono-) fractal scaling properties and the detection of long-range correlations in noisy, nonstationary time series [3-7]. It has successfully been applied to diverse fields such as DNA sequences [3,8], heart rate dynamics [9,10], neuron spiking [11], human gait [12], long-time weather records [13], cloud structure [14], geology [15], ethnology [16], economical time series [17], and solid state physics [18]. One reason to employ the DFA method is to avoid spurious detection of correlations that are artefacts of nonstationarity in time series.

The focus of the present paper is on the intriguing statistical properties and multifractal nature of the sunspot time series. In general, two different types of multifractality in time series can be distinguished: (i) Multifractality due to a fatness of probability density function (PDF) of the time series. In this case the multifractality cannot be removed by shuffling the series. (ii) Multifractality due to different long-range correlations in small and large scale fluctuations. In this case the data may have a PDF with finite moments, e. g. a Gaussian distribution. Thus the corresponding shuffled time series will exhibit mono-fractal scaling, since all long-range correlations are destroyed by the shuffling procedure. If both kinds of multifractality are present, the shuffled series will show weaker multifractality than the original series.

In some cases, there exist one or more crossover (time)

scales s_{\times} separating regimes with different scaling exponents [5,6]. In this case investigation of the scaling behavior is more complicate and different scaling exponents are required for different parts of the series [7]. Therefore one needs a multitude of scaling exponents (multifractality) for a full description of the scaling behavior.

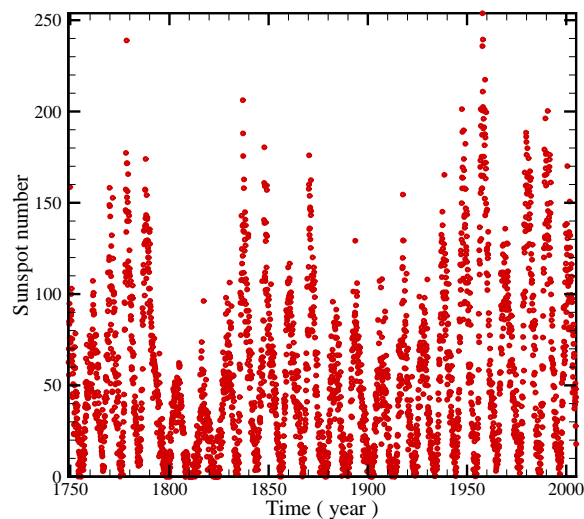


FIG. 1. Observed spot numbers as a function of time.

This paper is organized as follows: In Section II we describe the MF-DFA method in detail and show that the scaling exponents determined via the MF-DFA method are identical to those obtained by the standard multifractal formalism based on partition functions. The MF-DFA results of sunspot time series and crossover time scale are presented in Section III. In Section IV, we show that the long-range correlation is dominant by comparing the MF-DFA results for original series to those obtained via the MF-DFA for shuffled and surrogate series. Section V closes with a discussion of the present results.

II. MULTIFRACTAL DETRENDED FLUCTUATION ANALYSIS

The simplest type of the multifractal analysis is based upon the standard partition function multifractal formalism, which has been developed for the multifractal characterization of normalized, stationary measurements [19–22]. Unfortunately, this standard formalism does not give correct results for non-stationary time series that are affected by trends or that cannot be normalized. Thus, in the early 1990s an improved multifractal formalism has been developed, the wavelet transform modulus maxima (WTMM) method [23], which is based on the wavelet analysis and involves tracing the maxima lines in the continuous wavelet transform over all scales. Here, we apply an alternative approach based on a generalization of the DFA method for the analysis of sunspot time series. This multifractal DFA (MF-DFA) does not require the modulus maxima procedure, and hence does not require more effort in programming and computing than the conventional DFA.

A. Description of the MF-DFA

The generalized multifractal DFA (MF-DFA) procedure consists of five steps. The first three steps are essentially identical to the conventional DFA procedure (see e. g. [3–7]). Suppose that x_k is a series of length N , and that this series is of compact support, i.e. $x_k = 0$ for an insignificant fraction of the values only.

- *Step 1:* Determine the “profile”

$$Y(i) \equiv \sum_{k=1}^i [x_k - \langle x \rangle], \quad i = 1, \dots, N. \quad (1)$$

Subtraction of the mean $\langle x \rangle$ is not compulsory, since it would be eliminated by the later detrending in the third step.

- *Step 2:* Divide the profile $Y(i)$ into $N_s \equiv \text{int}(N/s)$ non-overlapping segments of equal lengths s . Since the length N of the series is often not a multiple of the considered time scale s , a short part at the end of the profile may remain. In order not to disregard this part of the series, the same procedure is repeated starting from the opposite end. Thereby, $2N_s$ segments are obtained altogether.

- *Step 3:* Calculate the local trend for each of the $2N_s$ segments by a least-square fit of the series. Then determine the variance

$$F^2(s, \nu) \equiv \frac{1}{s} \sum_{i=1}^s \{Y[(\nu - 1)s + i] - y_\nu(i)\}^2 \quad (2)$$

for each segment ν , $\nu = 1, \dots, N_s$ and

$$F^2(s, \nu) \equiv \frac{1}{s} \sum_{i=1}^s \{Y[N - (\nu - N_s)s + i] - y_\nu(i)\}^2 \quad (3)$$

for $\nu = N_s + 1, \dots, 2N_s$. Here, $y_\nu(i)$ is the fitting polynomial in segment ν . Linear, quadratic, cubic, or higher order polynomials can be used in the fitting procedure (conventionally

called DFA1, DFA2, DFA3, . . .) [3,10]. Since the detrending of the time series is done by the subtraction of the polynomial fits from the profile, different order DFA differ in their capability of eliminating trends in the series. In (MF-)DFA m [m th order (MF-)DFA] trends of order m in the profile (or, equivalently, of order $m - 1$ in the original series) are eliminated. Thus a comparison of the results for different orders of DFA allows one to estimate the type of the polynomial trend in the time series [5,6].

- *Step 4:* Average over all segments to obtain the q -th order fluctuation function, defined as:

$$F_q(s) \equiv \left\{ \frac{1}{2N_s} \sum_{\nu=1}^{2N_s} [F^2(s, \nu)]^{q/2} \right\}^{1/q}, \quad (4)$$

where, in general, the index variable q can take any real value except zero. For $q = 2$, the standard DFA procedure is retrieved. Generally we are interested in how the generalized q dependent fluctuation functions $F_q(s)$ depend on the time scale s for different values of q . Hence, we must repeat steps 2, 3 and 4 for several time scales s . It is apparent that $F_q(s)$ will increase with increasing s . Of course, $F_q(s)$ depends on the DFA order m . By construction, $F_q(s)$ is only defined for $s \geq m + 2$.

- *Step 5:* Determine the scaling behavior of the fluctuation functions by analyzing log-log plots of $F_q(s)$ versus s for each value of q . If the series x_i are long-range power-law correlated, $F_q(s)$ increases, for large values of s , as a power-law,

$$F_q(s) \sim s^{h(q)}. \quad (5)$$

In general, the exponent $h(q)$ may depend on q . For stationary time series, $0 < h(2) < 1.0$, where $h(2)$ is identical to the well-known Hurst exponent H (see e. g. [19]). In the non-stationary case the corresponding scaling exponent of $F_q(s)$ is identified by $\bar{\alpha}(q) > 1.0$. It is converted into the Hurst exponent according to $H = \bar{\alpha}(q = 2) - 1$. Thus, one can call the function $h(q)$ the generalized Hurst exponent.

For monofractal time series, $h(q)$ is independent of q , since the scaling behavior of the variances $F^2(s, \nu)$ is identical for all segments ν , and the averaging procedure in Eq. (4) will just give this identical scaling behavior for all values of q . If we consider positive values of q , the segments ν with large variance $F_s^2(\nu)$ (i. e. large deviations from the corresponding fit) will dominate the average $F_q(s)$. Thus, for positive values of q , $h(q)$ describes the scaling behavior of the segments with large fluctuations. For negative values of q , the segments ν with small variance $F_s^2(\nu)$ will dominate the average $F_q(s)$. Hence, for negative values of q , $h(q)$ describes the scaling behavior of the segments with small fluctuations [24].

B. Relation to standard multifractal analysis

For a stationary, normalized series the multifractal scaling exponents $h(q)$ defined in Eq. (5) are directly related to the scaling exponents $\tau(q)$ defined by the standard partition

function-based multifractal formalism as shown below. Suppose that the series x_k of length N is a stationary, normalized sequence. Then the detrending procedure in step 3 of the MF-DFA method is not required, since no trend has to be eliminated. Thus, the DFA can be replaced by the standard Fluctuation Analysis (FA), which is identical to the DFA except for a simplified definition of the variance for each segment ν , $\nu = 1, \dots, N_s$. Step 3 now becomes [see Eq. (2)]:

$$F_{\text{FA}}^2(s, \nu) \equiv [Y(\nu s) - Y((\nu - 1)s)]^2. \quad (6)$$

Inserting this simplified definition into Eq. (4) and using Eq. (5), we obtain

$$\left\{ \frac{1}{2N_s} \sum_{\nu=1}^{2N_s} |Y(\nu s) - Y((\nu - 1)s)|^q \right\}^{1/q} \sim s^{h(q)}. \quad (7)$$

For simplicity we can assume that the length N of the series is an integer multiple of the scale s , obtaining $N_s = N/s$ and therefore

$$\sum_{\nu=1}^{N/s} |Y(\nu s) - Y((\nu - 1)s)|^q \sim s^{qh(q)-1}. \quad (8)$$

This corresponds to the multifractal formalism used e. g. in [20,22]. In fact, a hierarchy of exponents H_q similar to our $h(q)$ has been introduced based on Eq. (8) in [20]. In order to relate also to the standard textbook box counting formalism [19,21], we employ the definition of the profile in Eq. (1). It is evident that the term $Y(\nu s) - Y((\nu - 1)s)$ in Eq. (8) is identical to the sum of the numbers x_k within each segment ν of size s . This sum is known as the box probability $p_s(\nu)$ in the standard multifractal formalism for normalized series x_k ,

$$p_s(\nu) \equiv \sum_{k=(\nu-1)s+1}^{\nu s} x_k = Y(\nu s) - Y((\nu - 1)s). \quad (9)$$

The scaling exponent $\tau(q)$ is usually defined via the partition function $Z_q(s)$,

$$Z_q(s) \equiv \sum_{\nu=1}^{N/s} |p_s(\nu)|^q \sim s^{\tau(q)}, \quad (10)$$

where q is a real parameter as in the MF-DFA method, discussed above. Using Eq. (9) we see that Eq. (10) is identical to Eq. (8), and obtain analytically the relation between the two sets of multifractal scaling exponents,

$$\tau(q) = qh(q) - 1. \quad (11)$$

Thus, we observe that $h(q)$ defined in Eq. (5) for the MF-DFA is directly related to the classical multifractal scaling exponents $\tau(q)$. Note that $h(q)$ is different from the generalized multifractal dimensions

$$D(q) \equiv \frac{\tau(q)}{q-1} = \frac{qh(q) - 1}{q-1}, \quad (12)$$

that are used instead of $\tau(q)$ in some papers. While $h(q)$ is independent of q for a monofractal time series, $D(q)$ depends on q in this case. Another way to characterize a multifractal series is the singularity spectrum $f(\alpha)$, that is related to $\tau(q)$ via a Legendre transform [19,21],

$$\alpha = \tau'(q) \quad \text{and} \quad f(\alpha) = q\alpha - \tau(q). \quad (13)$$

Here, α is the singularity strength or Hölder exponent, while $f(\alpha)$ denotes the dimension of the subset of the series that is characterized by α . Using Eq. (11), we can directly relate α and $f(\alpha)$ to $h(q)$,

$$\alpha = h(q) + qh'(q) \quad \text{and} \quad f(\alpha) = q[\alpha - h(q)] + 1. \quad (14)$$

A Hölder exponent denotes monofractality, while in the multifractal case, the different parts of the structure are characterized by different values of α , leading to the existence of the spectrum $f(\alpha)$.

III. ANALYSIS OF SUNSPOT TIME SERIES

As mentioned in section II, generalized Hurst exponents $h(q)$ in Eq. (5) can be found by analyzing log-log plots of $F_q(s)$ versus s for each q . Our investigation shows that there is at least one crossover time scale s_\times in the log-log plots of $F_q(s)$ versus s for every q 's, for a monthly time axis. Figure 2 shows that there are different scaling exponent for time scales $s > s_\times$ and $s < s_\times$. To ensure the existence of the crossover time scale, we plot the log-log graph of $F_q(s)$ versus s for $q = -1.0$, $q = 2.0$ and $q = 3.0$ in figure 3. This proves that existence of the crossover time scale do not depend on the special values of q . The crossover time scale is about $s_\times \sim 130$ which is equal to the well known cycle of approximately 11 years of sun activity.

Let us now apply MF-DFA1 method for two different time scales i.e. $s < 130$ and $s > 130$. Figure 4 shows the MF-DFA1 results for time scale $s > 130$. The signal is *almost* monofractal which means that $h(q)$ dose not vary significantly with q . The weak q -dependence of $h(q)$ is shown in Figure 4, but q -dependence of the classical multifractal scaling exponent $\tau(q)$ has different behaviors for $q < 0$ and $q > 0$. For positive and negative values of q , the slopes of $\tau(q)$ are 0.55 ± 0.001 and 0.33 ± 0.001 , respectively. According to the relation between the Hurst exponent and $h(2)$, i.e. $h(q = 2) = H$, we find that the Hurst exponent is 0.62 ± 0.04 . This means that the sunspot time series in time scales $s > s_\times$ is a stationary process with long-range correlation [25].

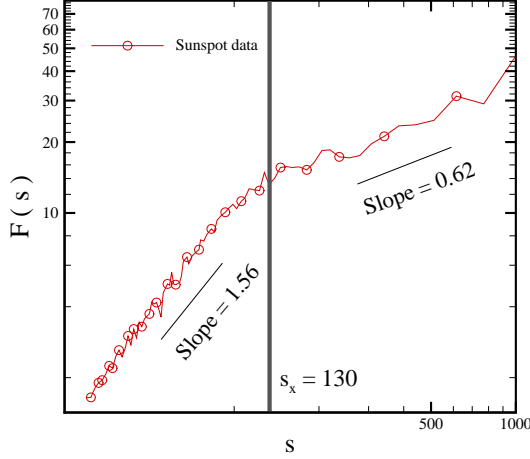


FIG. 2. Crossover time scale in correlation behavior for sunspot time series in log-log plot $F(s)$ versus s for $q = 2.0$.

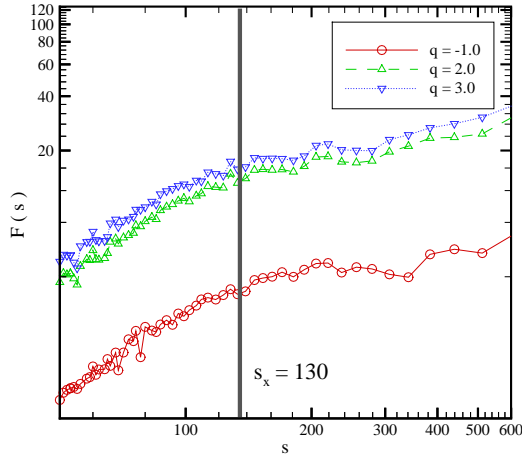


FIG. 3. The MF-DFA1 functions $F_q(s)$ for sunspot time series are shown versus the time scale s in log-log plot for $q = -1.0$, $q = 2.0$ and $q = 3.0$.

The auto-correlation function can be characterized by a power law $C(s) \equiv \langle n_k n_{k+s} \rangle \sim s^{-\gamma}$ with exponent $\gamma = 2 - 2H$. Its power spectra can be characterized by $S(\omega) \sim \omega^{-\beta}$ with frequency ω and $\beta = 2H - 1$. The singularity spectrum $f(\alpha)$, Eq. (13) is shown in Figure 4. All the related quantities are given in Table I and Table II.

The MF-DFA1 results for monthly sunspot time series for time scales $s < 130$ are shown in Figure 5. Sunspot time series in this regime is a multifractal process as indicated by the strong q dependence of generalized Hurst exponent and $\tau(q)$. The upper and lower slopes of $\tau(q)$ as a function of q are 0.13 ± 0.001 and 1.56 ± 0.001 , respectively. The gen-

eralized Hurst exponent is $\bar{\alpha}(q = 2) = 1.59 \pm 0.03$, and indicates that this process for the time scales $s < 130$ is a nonstationary process with long-range correlation behavior. The auto-correlation function and power spectra exponents are $\gamma = -2H$ and $\beta = 2H + 1$, respectively [26,27]. The fractal dimension in this regime is obtained as $D_f = 2 - H = 1.44$ [5]. The values of derived quantities from MF-DFA1 method, are given in Table III and Table IV.

IV. COMPARISON OF THE MULTIFRACTALITY FOR ORIGINAL, SHUFFLED AND SURROGATE SUNSPOT TIME SERIES

As mentioned in the introduction, two different types of multifractality in time series can be distinguished. In both cases is required a multitude of scaling exponents for small and large fluctuations. In this section we interested in the nature of the multifractal behavior of sunspot time series. The origin of multifractality of a time series can be due to the broadness (fatness) of probability density function (PDF) of sunspot time series or due to the different long-range correlations of the number fluctuations. Here we would like to distinguish between these two types of multifractality. The easiest way to clarify this question is to analysis the corresponding shuffled and surrogate series. The shuffling of time series destroys the long range correlation, Therefore if the multifractality only belongs to the long range correlation, we should find $h_{\text{shuf}}(q) = 0.5$. The multifractality nature due to the fatness of the PDF signals is not affected by the shuffling procedure.

In the surrogate method, the phase of discrete fourier transform (DFT) coefficients of sunspot time series are replaced with a set of pseudo independent distributed uniform $(-\pi, \pi)$ quantities. The correlations in the surrogate series do not change, but the probability function changes to the Gaussian distribution. If multifractality in the time series is due to a broad PDF, $h(q)$ obtained by the surrogate method will be independent of q . If both kinds of multifractality are present in sunspot time series, the shuffled and surrogate series will show weaker multifractality than the original one.

To check the nature of multifractality, we compare the fluctuation function $F_q(s)$, for the original series with the result of the corresponding shuffled, $F_q^{\text{shuf}}(s)$ and surrogate series $F_q^{\text{sur}}(s)$. Differences between these two fluctuation functions with the original one, directly indicate the presence of long range correlations or broadness of probability density function in the original series. These differences can be observed in a plot of the ratio $F_q(s)/F_q^{\text{shuf}}(s)$ and $F_q(s)/F_q^{\text{sur}}(s)$ versus s [25]. Since the anomalous scaling due to a broad probability density affects $F_q(s)$ and $F_q^{\text{shuf}}(s)$ in the same way, only multifractality due to correlations will be observed in $F_q(s)/F_q^{\text{shuf}}(s)$. The scaling behavior of these ratios are

$$F_q(s)/F_q^{\text{shuf}}(s) \sim s^{h(q)-h_{\text{shuf}}(q)} = s^{h_{\text{cor}}(q)}. \quad (15)$$

$$F_q(s)/F_q^{\text{sur}}(s) \sim s^{h(q)-h_{\text{sur}}(q)} = s^{h_{\text{PDF}}(q)}. \quad (16)$$

If only fatness of the PDF is responsible for the multifractality, one should find $h(q) = h_{\text{shuf}}(q)$ and $h_{\text{cor}}(q) = 0$. On the other hand, deviations from $h_{\text{cor}}(q) = 0$ indicates the presence of correlations, and q dependence of $h_{\text{cor}}(q)$ indicates that multifractality is due to the long range correlation. If only correlation multifractality is present, one finds $h_{\text{shuf}}(q) = 0.5$. If both distribution and correlation multifractality are present, both, $h_{\text{shuf}}(q)$ and $h_{\text{sur}}(q)$ will depend on q .

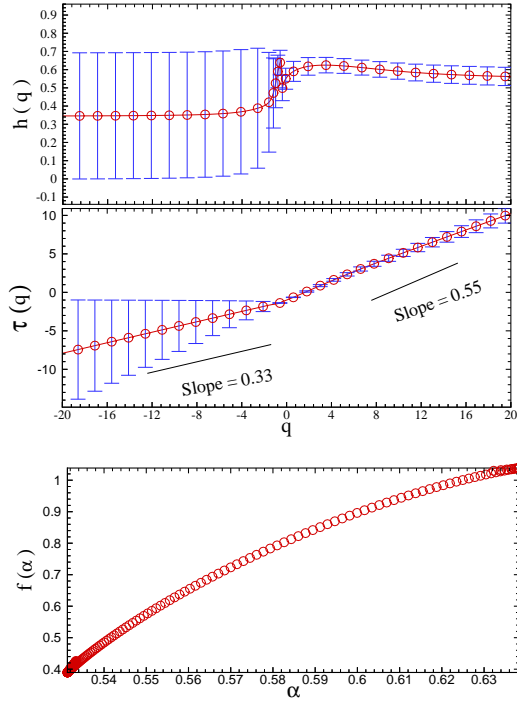


FIG. 4. The q dependence of the generalized Hurst exponent $h(q)$, the corresponding $\tau(q)$ and singularity spectrum $f(\alpha)$ determined by fits on scales $s > s_x$ are shown in the upper to lower panel respectively for original sunspot time series.

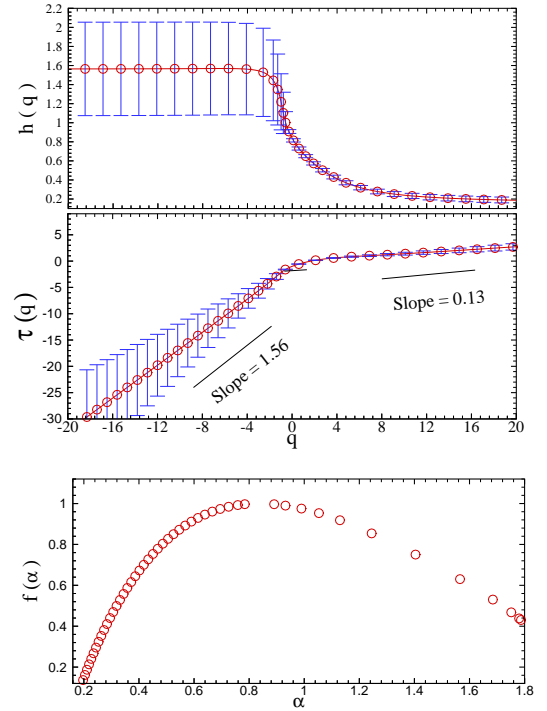


FIG. 5. The q dependence of the generalized Hurst exponent $\bar{\alpha}(q)$, the corresponding $\tau(q)$ and singularity spectrum $f(\alpha)$ determined by fits on scales $s < s_x$ are shown in the upper to lower panel respectively for original sunspot time series.

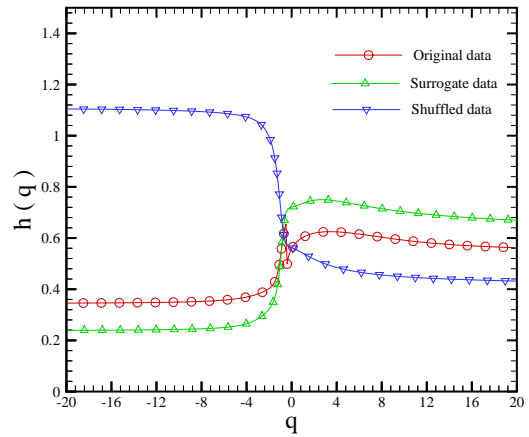


FIG. 6. $h(q)$ as a function of q in the $s > s_x$ regime for original, surrogate and shuffled data.

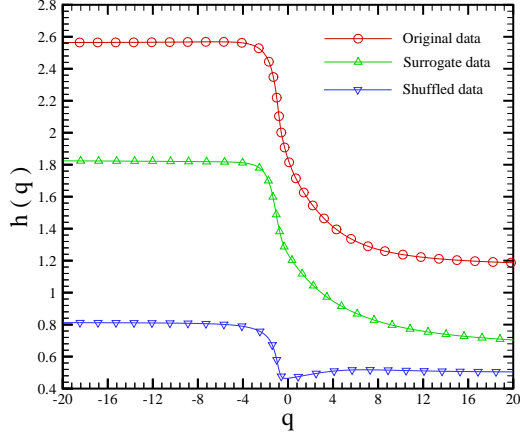


FIG. 7. Generalized Hurst exponent as a function of q in the $s < s_{\times}$ regime for original, surrogate and shuffled data.

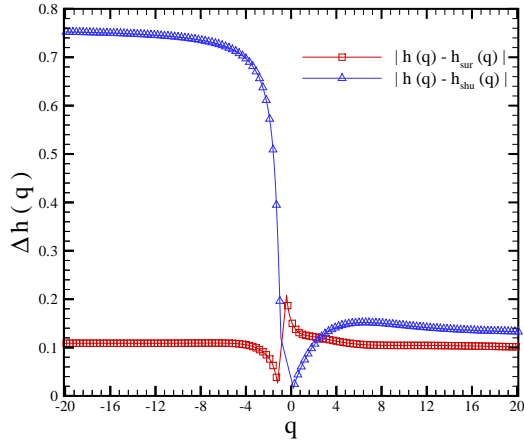


FIG. 8. Absolute values of $h_{cor} = h(q) - h_{shu}(q)$ and $h_{PDF} = h(q) - h_{sur}(q)$ as a function of q for $s > s_{\times}$ time scales .

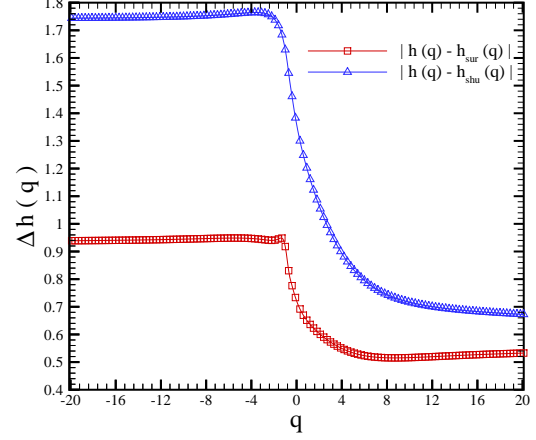


FIG. 9. Absolute values of $h_{cor} = h(q) - h_{shu}(q)$ and $h_{PDF} = h(q) - h_{sur}(q)$ as a function of q for $s < s_{\times}$ time scales .

The q dependence of the exponent $h(q)$ for original, surrogate and shuffled time series are shown in Figures 6 and 7. Also the exponent h_{cor} and h_{PDF} vs q for time scales $s > s_{\times}$ and $s < s_{\times}$ are illustrated in Figures 8 and 9, respectively. The q dependence of h_{cor} and h_{PDF} shows that the multifractality nature of sunspot time series is due to both broadness of the PDF and long range correlation. In both cases the absolute value of $h_{cor}(q)$ is greater than $h_{PDF}(q)$, so the multifractality due to the fatness is weaker than the multifractality due to the correlation. The deviation of $h_{cor}(q)$ and $h_{PDF}(q)$ from $h(q)$ can be determined by using χ^2_{ν} test as follows:

$$\chi^2_{\nu} = \frac{1}{N-m} \sum_{i=1}^N \frac{[h(q) - h_{\diamond}(q)]^2}{\sigma(q)^2 + \sigma_{\diamond}(q)^2}, \quad (17)$$

where $N-m$ is the degree of freedom and the symbol \diamond can be replaced by *cor* and *PDF* to determine the confidence level of h_{shu} and h_{sur} to generalized Hurst exponents of original series, respectively. The value of χ^2_{ν} for shuffled and surrogate time series in the $s > s_{\times}$ and $s < s_{\times}$ regimes are 3.41, 1.33 and 569.00, 102.38, respectively. In Figure 10 we compare the dependence of $F(s)$ to the scale s for the original, surrogate and shuffled sunspot time series. As we mentioned above the effect of shuffled series on the MF-DFA1 results is greater than surrogate series.

The crossover time scale in correlation behavior in the shuffled series is destroyed, however this time scale exists in the surrogate series.

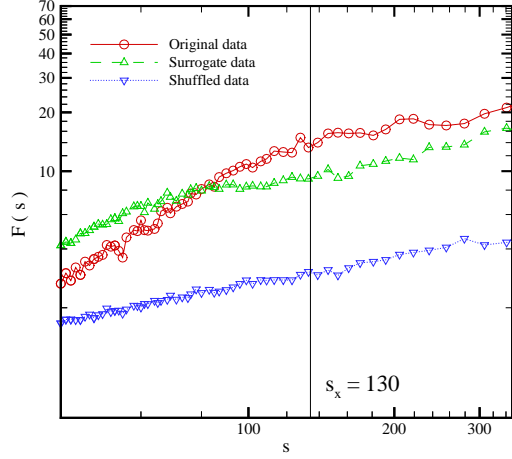


FIG. 10. The log-log plots of the standard MF-DFA1 function $F(s)$ versus the time scale s for the original, surrogate and shuffled sunspot time series.

The values of the Hurst exponent H , multifractal scaling $\tau(q = 2)$ and generalized multifractal exponents ($D(q = 2)$) for the time scales ($s > s_\times$) of the original, shuffled and surrogate of sunspot time series obtained with MF-DFA1 method are reported in Table I, The related scaling exponents are indicated in Table II. The MF-DFA1 results for time scales $s < s_\times$ are reported in Tables III and IV.

TABLE I. The values of the Hurst, multifractal scaling and generalized multifractal exponents for $q = 2.0$ for time scales ($s > s_\times$) for original, surrogate and shuffled of monthly sunspot time series obtained by MF-DFA1.

Data	H	τ	D
Sunspot	0.62 ± 0.04	0.24 ± 0.08	0.24 ± 0.08
Surrogate	0.74 ± 0.03	0.48 ± 0.06	0.48 ± 0.06
Shuffled	0.51 ± 0.03	0.02 ± 0.06	0.02 ± 0.06

TABLE II. The values of the Hurst (H), power spectrum scaling ($\beta = \tau(q = 2)$) and auto-correlation scaling (γ) exponents for time scales ($s > s_\times$) for original, surrogate and shuffled of monthly sunspot time series obtained by MF-DFA1.

Data	H	β	γ
Sunspot	0.62 ± 0.04	0.24 ± 0.08	0.76 ± 0.08
Surrogate	0.74 ± 0.03	0.48 ± 0.06	0.52 ± 0.06
Shuffled	0.51 ± 0.03	0.02 ± 0.06	0.98 ± 0.06

TABLE III. The values of $\bar{\alpha}$, multifractal scaling and generalized multifractal exponents for $q = 2.0$ for time scales ($s < s_\times$) for original, surrogate and shuffled of monthly sunspot time series obtained by MF-DFA1.

Data	$\bar{\alpha}$	τ	D
Sunspot	1.56 ± 0.02	0.12 ± 0.04	0.12 ± 0.04
Surrogate	0.96 ± 0.03	0.92 ± 0.06	0.92 ± 0.06
Shuffled	0.50 ± 0.001	0.00 ± 0.002	0.00 ± 0.002

TABLE IV. The values of the Hurst (H), power spectrum scaling (β) and auto-correlation scaling (γ) exponents in time scales ($s < s_\times$) for original, surrogate and shuffled of monthly sunspot time series obtained by MF-DFA1.

Data	H	β	γ
Sunspot	0.56 ± 0.02	2.12 ± 0.04	-1.12 ± 0.04
Surrogate	0.96 ± 0.03	0.92 ± 0.06	0.08 ± 0.06
Shuffled	0.50 ± 0.001	0.00 ± 0.002	1.00 ± 0.004

V. CONCLUSION

The MF-DFA method allows us to determine the multifractal characterization of the nonstationary and stationary time series. We have shown that the monthly sunspot time series has a crossover time scale (s_{\times}). This crossover time scale is equal to the well known cycle of sun activity, approximately 11 years(132 months). Applying the MF-DFA1 method shows that the monthly sunspot time series is an effectively stationary time series for time scales $s > s_{\times}$ and a nonstationary process for $s < s_{\times}$. The weak q dependence of $h(q)$ and $\tau(q)$, for the $s > s_{\times}$ shows that the monthly sunspot time series has an almost monofractal behavior. Otherwise for $s < s_{\times}$, the strong q dependence of $h(q)$ and $\tau(q)$, indicates that the sunspot number fluctuation is a multifractal. By comparing the generalized Hurst exponent of the original time series with the shuffled and surrogate one's, we have found that multifractality due to the correlation has more contribution than the broadness of the probability density function. We have estimated also the Hurst exponent in small and large time scales via the modified MF-DFA method. Usually, in the MF-DFA method, deviation from a straight line in the log-log plot of Eq. (5) occurs for small scales s . This deviation limits the capability of DFA to determine the correct correlation behavior for very short scales and in the regime of small s . The modified MF-DFA is defined as follows [5]:

$$F_q^{\text{mod}}(s) = \frac{F_q(s)}{K_q(s)} = F_q(s) \frac{\langle [F_q^{\text{shuf}}(s')]^2 \rangle^{1/2} s^{1/2}}{\langle [F_q^{\text{shuf}}(s)]^2 \rangle^{1/2} s^{1/2}} \quad (\text{for } s' \gg 1), \quad (18)$$

where $\langle [F_q^{\text{shuf}}(s)]^2 \rangle^{1/2}$ denotes the usual MF-DFA fluctuation function [defined in Eq. (4)] averaged over several configurations of shuffled data taken from the original time series, and $s' \approx N/40$. The values of the Hurst exponent obtained by MF-DFA1 and modified MF-DFA1 methods are given in Table V. The relative deviation of the Hurst exponent which is obtained by modified MF-DFA1 in comparison to MF-DFA1 in the $s < s_{\times}$ regime, is approximately 7.14% for original sunspot time series.

TABLE V. The value of the Hurst exponent using MF-DFA1 and modified MF-DFA1 for the original, shuffled and surrogate of monthly sunspot time series.

Regime	Method	Sunspot	Surrogate	Shuffled
$s > s_{\times}$	MF-DFA1	0.62 ± 0.04	0.74 ± 0.03	0.51 ± 0.03
$s > s_{\times}$	Modified	0.62 ± 0.04	0.73 ± 0.05	0.52 ± 0.03
$s < s_{\times}$	MF-DFA1	0.56 ± 0.02	0.96 ± 0.03	0.50 ± 0.001
$s < s_{\times}$	Modified	0.6 ± 0.02	0.94 ± 0.03	0.51 ± 0.01

Acknowledgements

We would like to thank Sepehr Arbabi Bidgoli for reading the manuscript and useful comments.

-
- [1] see for example *Sunspots* by R.J. Bray, R.E. Loughhead, Dover Publications, New York 1979.
 - [2] <http://www.oma.be/KSB-ORB/SIDC/index.html>
 - [3] C.-K. Peng, S. V. Buldyrev, S. Havlin, M. Simons, H. E. Stanley, and A. L. Goldberger, Phys. Rev. E **49**, 1685 (1994); S. M. Ossadnik, S. B. Buldyrev, A. L. Goldberger, S. Havlin, R.N. Mantegna, C.-K. Peng, M. Simons, and H.E. Stanley, Biophys. J. **67**, 64 (1994).
 - [4] M. S. Taqqu, V. Teverovsky, and W. Willinger, Fractals **3**, 785 (1995).
 - [5] J. W. Kantelhardt, E. Koscielny-Bunde, H. H. A. Rego, S. Havlin, and A. Bunde, Physica A **295**, 441 (2001).
 - [6] K. Hu, P. Ch. Ivanov, Z. Chen, P. Carpena, and H. E. Stanley, Phys. Rev. E **64**, 011114 (2001).
 - [7] Z. Chen, P. Ch. Ivanov, K. Hu, and H. E. Stanley, Phys. Rev. E **65**, (April 2002), preprint physics/0111103.
 - [8] S. V. Buldyrev, A. L. Goldberger, S. Havlin, R. N. Mantegna, M. E. Matsa, C.-K. Peng, M. Simons, and H. E. Stanley, Phys. Rev. E **51**, 5084 (1995); S. V. Buldyrev, N. V. Dokholyan, A. L. Goldberger, S. Havlin, C.-K. Peng, H. E. Stanley, and G. M. Viswanathan, Physica A **249**, 430 (1998).
 - [9] C.-K. Peng, S. Havlin, H. E. Stanley, and A. L. Goldberger, Chaos **5**, 82 (1995); P. Ch. Ivanov, A. Bunde, L. A. N. Amaral, S. Havlin, J. Fritsch-Yelle, R. M. Baevsky, H. E. Stanley, and A. L. Goldberger, Europhys. Lett. **48**, 594 (1999); Y. Ashkenazy, M. Lewkowicz, J. Levitan, S. Havlin, K. Saermark, H. Moelgaard, P. E. B. Thomsen, M. Moller, U. Hintze, and H. V. Huikuri, Europhys. Lett. **53**, 709 (2001); Y. Ashkenazy, P. Ch. Ivanov, S. Havlin, C.-K. Peng, A. L. Goldberger, and H. E. Stanley, Phys. Rev. Lett. **86**, 1900 (2001).
 - [10] A. Bunde, S. Havlin, J. W. Kantelhardt, T. Penzel, J.-H. Peter, and K. Voigt, Phys. Rev. Lett. **85**, 3736 (2000).
 - [11] S. Blesic, S. Milosevic, D. Stratimirovic, and M. Ljubisavljevic, Physica A **268**, 275 (1999); S. Bahar, J. W. Kantelhardt, A. Neiman, H. H. A. Rego, D. F. Russell, L. Wilkens, A. Bunde, and F. Moss, Europhys. Lett. **56**, 454 (2001).
 - [12] J. M. Hausdorff, S. L. Mitchell, R. Firtion, C.-K. Peng, M. E. Cudkowicz, J. Y. Wei, and A. L. Goldberger, J. Appl. Physiology **82**, 262 (1997).
 - [13] E. Koscielny-Bunde, A. Bunde, S. Havlin, H.E. Roman, Y. Goldreich, and H.-J. Schellnhuber, Phys. Rev. Lett. **81**, 729 (1998). K. Ivanova and M. Ausloos, Physica A **274**, 349 (1999); P. Talkner and R.O. Weber, Phys. Rev. E **62**, 150 (2000).
 - [14] K. Ivanova, M. Ausloos, E. E. Clothiaux, and T. P. Ackerman, Europhys. Lett. **52**, 40 (2000).
 - [15] B. D. Malamud and D. L. Turcotte, J. Stat. Plan. Infer. **80**, 173 (1999).
 - [16] C. L. Alados and M. A. Huffman, Ethnology **106**, 105 (2000).
 - [17] R. N. Mantegna and H. E. Stanley, *An Introduction to Econophysics* (Cambridge University Press, Cambridge, 2000); Y. Liu, P. Gopikrishnan, P. Cizeau, M. Meyer, C.-K. Peng, and

- H. E. Stanley, Phys. Rev. E **60**, 1390 (1999); N. Vandewalle, M. Ausloos, and P. Boveroux, Physica A **269**, 170 (1999).
- [18] J. W. Kantelhardt, R. Berkovits, S. Havlin, and A. Bunde, Physica A **266**, 461 (1999); N. Vandewalle, M. Ausloos, M. Houssa, P. W. Mertens, and M. M. Heyns, Appl. Phys. Lett. **74**, 1579 (1999).
- [19] J. Feder, *Fractals* (Plenum Press, New York, 1988).
- [20] A.-L. Barabási and T. Vicsek, Phys. Rev. A **44**, 2730 (1991).
- [21] H.-O. Peitgen, H. Jürgens, and D. Saupe, *Chaos and Fractals* (Springer-Verlag, New York, 1992), Appendix B.
- [22] E. Bacry, J. Delour, and J. F. Muzy, Phys. Rev. E **64**, 026103 (2001).
- [23] J. F. Muzy, E. Bacry, and A. Arneodo, Phys. Rev. Lett. **67**, 3515 (1991).
- [24] For the maximum scale $s = N$ the fluctuation function $F_q(s)$ is independent of q , since the sum in Eq. (4) runs over only two identical segments ($N_s \equiv [N/s] = 1$). For smaller scales $s \ll N$ the averaging procedure runs over several segments, and the average value $F_q(s)$ will be dominated by the $F^2(s, \nu)$ from the segments with small (large) fluctuations if $q < 0$ ($q > 0$). Thus, for $s \ll N$, $F_q(s)$ with $q < 0$ will be smaller than $F_q(s)$ with $q > 0$, while both become equal for $s = N$. Hence, if we assume an homogeneous scaling behavior of $F_q(s)$ following Eq. (5), the slope $h(q)$ in a log-log plot of $F_q(s)$ with $q < 0$ versus s must be larger than the corresponding slope for $F_q(s)$ with $q > 0$. Thus, $h(q)$ for $q < 0$ will usually be larger than $h(q)$ for $q > 0$.
- [25] J. W. Gantelhardt, S. A. Zschiegner, E. Koscielny-Bunde, A. Bunde, S. Pavlin and H. E. Stanley, Physica A **316**, 78-114 (2002).
- [26] C. K. Peng, S. Buldyrev, S. Havlin, M. Simons, H. Stanley and A. Goldberger, Phys. Rev. E. **49**, 1685-9 (1994).
- [27] A. Eke, P. Herman, L. Kocsis and L. R. Kozak, Physiol. Meas. **23**, R1-R38 (2002)
- [28] F. Pallikari, E. Boller, J. S. Exploration, **13**, 1, 25-40 (1999).